18th IFHTSE CONGRESS
International Federation for Heat Treatment and Surface Engineering
IFHTSE
ANAIS
PROCEEDINGS
ISSN 1516-392X

QUENCH RATE EFFECTS ON THE NATURAL AGING BEHAVIOR OF 7XXX AL-MG-ZN-CU ALUMINUM ALLOYS[1]

D. Scott MacKenzie[2]

Abstract

The effect of quench rate on the natural aging behavior was examined using microhardness, conductivity and the differential scanning calorimeter. The data indicated that GPZ formed during extended natural aging of 7075, while extended aging of 7050 resulted in the precipitation of η'.

[1] *Technical contribution to the 18th IFHTSE Congress - International Federation for Heat Treatment and Surface Engineering, 2010 July 26-30th, Rio de Janeiro, RJ, Brazil.*

[2] *Houghton International, Valley Forge, PA USA.*

INTRODUCTION

The aluminum alloy system Al-Zn-Mg-Cu is the mainstay of aluminum alloys used in the aerospace industry. This alloy system is being used in fatigue and fracture critical applications in military and commercial aircraft. With increasing applications, and shrinking budgets, it is important that the most performance be obtained from any alloy system. Strength, as well as affordability, must be achieved for modern aircraft applications.

An understanding of precipitation during quenching and aging can be understood by nucleation theory applied to diffusion controlled solid-state reactions.[1] The kinetics of precipitation during quenching are dependent on the degree of solute supersaturation and the diffusion rate. As an alloy is quenched, there is greater supersaturation (assuming no solute precipitates) and the diffusion rate decreases with decreasing temperature. When either the supersaturation or the diffusion rate is low, the precipitation rate is low. At intermediate temperatures, the amount of supersaturation is relatively high, as is the diffusion rate. Therefore the precipitation rate is the greatest at intermediate temperatures. The amount of time spent in this critical temperature range is governed by the quench rate and quench path.

Quenching, and the cooling effect of quenchants have been extensively studied.[2-5] The first systematic attempt to correlate properties to the quench rate in Al-Zn-Mg-Cu alloys was performed by Fink and Wiley[6] for thin (0.064") sheet. A Time-Temperature-Tensile Property curve was created and was probably the first instance of a TTT diagram for aluminum. It was determined that the critical temperature range for 75S is 400°C to 290°C. This is similar to the critical temperature range found for Al-Zn-Mg-Cu alloys.[7] At quench rates exceeding 450°C/sec., it was determined that maximum strength and corrosion resistance were obtained. At intermediate quench rates of 450 to 100°C/sec., the strength obtained is lowered (using the same age treatment), but the corrosion resistance was unaffected. Between 100°/sec and 20°C/sec, the strength decreased rapidly, and the corrosion resistance is at a minimum. At quench rates below 20°C/sec, the strength decreases rapidly, but the corrosion resistance improved.

After quenching, parts are generally artificially aged to produce either peak strength, or overaged to produce improved corrosion properties. This is a complex process, and requires an understanding of vacancies, and the interaction of precipitation and metastable phases. In general, the sequence of precipitation occurs by clustering of vacancies, formation of GP Zones; nucleation of η´; precipitation of η, and finally the coarsening of the precipitates.

The effect of quench rate on the formation of Frank and prismatic dislocation loops has been studied.[8-10] The number of dislocation loops increased when the specimens were water quenched. The formation of loops is promoted by a small amount of solute atoms, and this effect depends on the kind of solute atoms and the difference of atomic radii between the trace element and aluminum. As the difference in solute radii increases, the formation of loops is promoted.

As the Mg content in aluminum is increased, there is a decreasing dependence of the quench rate.[11] The density of dislocation loops is higher with increasing Mg content at the same aging temperature as the pure aluminum. This is due to the difference between the aluminum and magnesium atomic radii. It was concluded that Frank loops are formed from vacancy clusters[12] of approximately 10 vacancies.[13] As the density of dislocation loops increases, there is a finer and more uniform distribution of nucleation sites. These vacancy rich clusters, present

immediately after quenching, form ordered GP zones.[14-15] In addition, the formation rate of these GP zones is enhanced, because of the shorter distance solute atoms have to diffuse to a vacancy rich cluster or Frank Loop.

The kinetics of vacancy-rich cluster formations are changed radically by the presence of Mg and this is interpreted as diffusion of Zn atoms along Mg-vacancy couples.[16] These couples readily move throughout the matrix at room temperature, and there is a strong binding energy between vacancies and Mg atoms. Polmear[17] investigated the aging characteristics of ternary Al-Zn-Mg alloys and found that the aging process was greatly modified by the addition of Mg to the binary Al-Zn alloys. He attributed this to the clustering of zinc and magnesium atoms as suggested by atomic size and thermodynamics. At low temperatures, nucleation proceeds predominately by the migration of Zn atoms. The consensus is that during the growth of the GP zones, Mg + Zn or Mg + Zn + vacancy complexes play a role.[18-20]

Comparing the characteristic properties of different trace elements on the precipitate dimensions and density after aging showed[21] that a combination of high solute/vacancy binding energy and diffusivity was required to significantly affect the length, thickness, and density of η'. The mechanism by which these trace elements affect the microstructure is to reduce the number of quenched-in dislocation loops for heterogeneous nucleation of precipitates. The decreased number of nucleation sites leads to a prolonged matrix super-saturation, which causes an increase in the length, thickness, and density of η'.

After quenching, small diffuse clusters of solute atoms are formed[22,23] prior to the formation of GP Zones. This was first demonstrated by Guinier[24,25] and Preston.[26,27] GP zones and the vacancy rich clusters (VRC) with a critical solute concentration are η'nucleation sites.[28] The precipitation mechanism is VRC → η' for water quenched specimens, and GPZ → η' for direct and step quenched specimens.[29] The vacancy rich clusters are most likely Frank Loops at aging temperatures. Nucleation of η' precipitates occurs in the matrix when no excess vacancies are available; and on quenched-in vacancy clusters. GP zones were not observed to be nuclei for the equilibrium precipitates (η).[30] The critical temperature for η precipitation corresponds to the intersection of the temperature of the C-curves for η and the η´ phases and does not correspond to the GP zone solvus temperature.[31]

Staley[32] found that tensile strength and conductivity followed a sigmoidal curve in 7050 as a function of aging time that was subsequently followed by a linear portion. The sigmoidal curve was attributed to the formation of G.P. Zones. The linear portion of the curve was attributed to the growth of the G. P. zones. Two stages for GP zone formation have been found.[33] In the first stage, the kinetics can be described by Cottrell-Bilby[34] type kinetics.

Duration of this stage is strongly influenced by the aging temperature and the composition of the alloy. It was thought that the formation of GP zones starts by the clustering of Zn atoms. Shortly thereafter, Mg atoms join the clusters. The process proceeds by the formation of nuclei of zones on these clusters. It is rate controlled by the diffusion of Mg-vacancy couples. In the second stage, the GP zones are growing. The growth of these GP zones is slowed by the formation of coherency strains around the GP zones, and the decrease in supersaturation.

As discussed, GP Zones are thought to be precursors for the intermediate precipitate η'. Mukhopadhyay[35] found direct evidence of η' precipitating on pre-existing GP Zones. Using small angle scattering measurements, it was found that the size of the GP Zones was limited to approximately 35-40 Å[36] prior to the

formation of the intermediate precipitate η'. This led to the conclusion that there was a critical GP Zone size for the precipitation of η'.[37,36]

Precipitation processes in Al-Mg-Zn-Cu alloys can be divided into three different types[38-39,17] defined by the temperatures utilized. The first type is for alloys quenched and aged above the GP zone solvus. Since no GP zones are formed, no easy nuclei for precipitation occurs. A very coarse dispersion of precipitates occurs with nucleation of η' occurring primarily on dislocations. The second type is for alloys quenched and aged below the GP zone solvus. GP zones form continuously and grow to a size where η' precipitation can occur. Nucleation and precipitation of η' is not effected by the quenching process except when vacancy-rich clusters form. The third type are alloys quenched below the GP solvus, and aged above the GP solvus. The final dispersion of precipitates and the PFZ width is controlled by the nucleation treatment below the GP zone solvus. This is the common situation for commercial heat treatments, and is typical of the T73 and T76 Tempers.

When Al-Zn-Mg-Cu alloys are quenched slowly, solute depletion and the loss of vacancies occurs. This depresses the critical nucleation temperature. This indicates that the solute lost during slow quenching (and the associated loss of strength from the loss of solute) is not recoverable. This loss can be partially compensated by adjusting the first stage aging practice to a temperature that allows the GP zones to grow to a stable size. This can also be accomplished by slow heating rates to the first stage age temperature.[32]

In 7XXX Al-Zn-Mg-Cu alloys, several phases have been identified that occur as a function of precipitation sequence. Four precipitation sequences have been identified. These are:

$$\alpha_{sss} \Rightarrow S$$
$$\alpha_{sss} \Rightarrow T' \Rightarrow T$$
$$\alpha_{sss} \Rightarrow VRC \Rightarrow GPZ \Rightarrow \eta' \Rightarrow \eta$$
$$\alpha_{sss} \Rightarrow \eta$$

In the first precipitation sequence, the S phase, Al_2CuMg, is precipitated directly from the supersaturated solid solution. In the second precipitation sequence, an intermediate phase T´ occurs in the decomposition of the supersaturated solid solution. Bernole and Graf first observed this phase.[40]

In the third sequence of precipitation, the supersaturated solid solution decomposes to form vacancy-rich clusters, Guinier-Preston Zones, η' and then η. Guinier-Preston Zones have been inferred in Al-Zn-Mg alloys, based on small increases in electrical conductivity and an increase in hardness during the initial stages of aging.[17] The η' phase is an intermediate step toward the precipitation of the equilibrium phase η ($MgZn_2$).

The fourth sequence generally occurs during slow quenching, or when aging temperatures are significantly above the GP-solvus.

Review of the literature indicates that there is a dispute over the occurrence of η' and its nucleation.[46,41,39,11,42-45] This leads to the speculation that the formation of η' is path dependant, and subject to local chemical variations. Mondolfo et al.[46] and others[47] indicate that nucleation of η' occurs by the segregation of alloying elements to stacking faults (Frank Loops), gradually losing coherency until the ordered η phase develops.[48] Others indicate that the formation of η' is the result of vacancy-rich clusters (VRC),[19,18] unless the temperature is greater than 100°C, in which

case, it is the result of Frank Loops. GP zones are also thought to nucleate η'.[49,45,37,50]

The kinetics of precipitation during artificial aging, measured by yield strength and conductivity, obey an Arrhenius relationship and indicate that the activation energies of 7075 and 7050 are similar.[32] The higher strength by aging at higher temperatures for 7050 was attributed to the effect of copper increasing the G.P. Zone solvus.

The kinetics of a reaction can be examined using the Johnson-Mehl-Avrami equation:[51-52]

$$V_f = 1 - \exp\left[-(kt)^n\right]$$

where V_f is the fraction transformed, k is a rate constant (sec^{-1}), and n is the Avrami exponent. This exponent contains information regarding the type of kinetics are occurring.[51] The rate constant k is described by:

$$k = k_0 e^{-\frac{Q}{RT}}$$

where Q is the activation energy for transformation, T is the temperature (°K) and R is the gas constant. The fraction transformed, V_f is described by:[53]

$$V_f = \frac{\rho(t) - \rho_i}{\rho_f - \rho_i}$$

where ρ is the property measured, and the subscripts indicate either the initial or final value of the property.

The assumptions in the Johnson-Mehl-Avrami equation are that nucleation and growth occurs simultaneously during the transformation. In addition, the nucleation of precipitates is homogeneously distributed throughout the matrix. It was also assumed that the nucleation rate was constant during the transformation process.

EXPERIMENTAL PROCEDURE

7075 and 7050 Jominy End Quench specimens were solution heat-treated at 480°C for two hours. These specimens were quenched, and allowed to naturally age for 1, 10, and 1000 hours. Hardness and conductivity measurements were taken as a function of time on the specimens naturally aged for 1000 hours.

RESULTS

The microstructures of naturally aged 7075 and 7050, quenched under different conditions were examined The 7075 water quenched specimens showed some precipitation at the longitudinal grain boundaries. There was little etching of the grain boundaries in the 7050 water-quenched specimens.

For both 7075 and 7050, as the quench rate decreased, there was more precipitation evident at the grain boundaries and in the interior of the grains. Evidence of precipitation on subgrain boundaries was observed in 7050. At the slowest cooling rate, copious precipitation has occurred. The precipitates that have formed are large, and have precipitated on grain boundaries and in the interior of grains. The microstructure has the appearance of an annealed aluminum structure.

The 7075 hardness results (Figure 1) show similar slopes toward the quenched end as 7050. Only two regions of hardening were observed. During the initial natural aging, 7075 exhibited a slight growth in hardness for the first 27 hours. This

was followed by a more rapid increase in the hardness. The rate of hardening from approximately 27 hours to the final hardness reading was nearly identical. The initial rate of response was more rapid as the quench rate was increased.

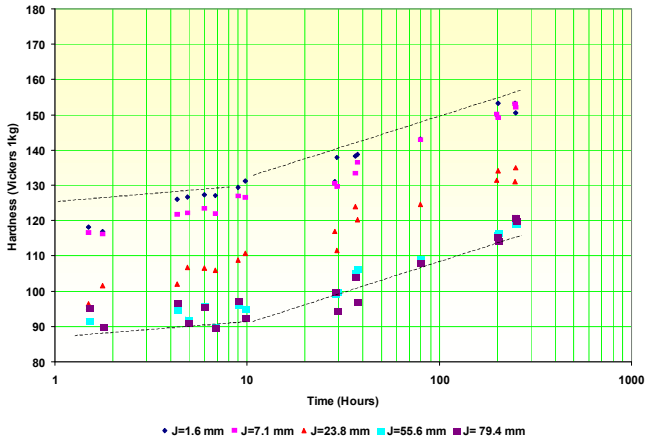

Figure 1. Aggregate natural hardening data for 7075.

The 7050 hardeness results (Figure 2), taken in aggregate, suggested that three stages of hardening occur. To approximately 10 hours after quench, all positions on the 7050 Jominy End Quench specimen harden at the same rate. After approximately 10 hours, a hardness plateau occurred until approximately 27 hours. After 27 hours, hardness again increases. Hardening occurs at the same rate at all positions.

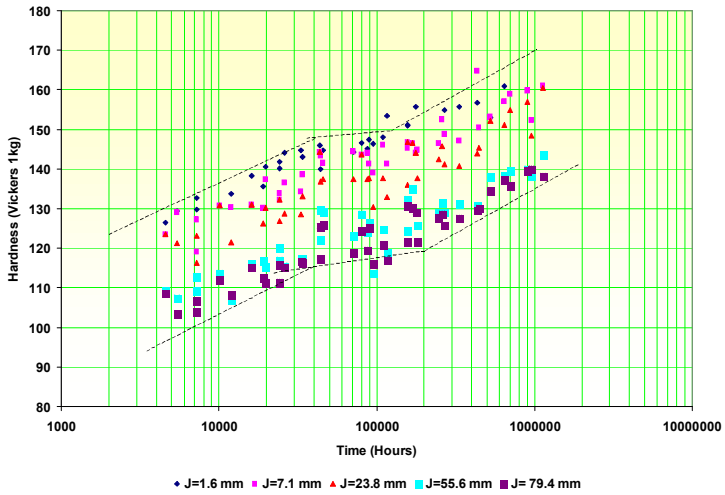

Figure 2. Aggregate natural hardening data for 7050.

Irrespective of the quench rate, 7075 and 7050 showed different responses during natural aging. This suggests a fundamental difference in the natural aging response and precipitation sequence of the two alloys.

The conductivity results for 7050 and 7075 exhibited similar behavior, and showed a decrease in the conductivity as the specimens naturally aged. A rapid decrease in the conductivity occurred until approximately 12 hours. After 12 hours, the change in conductivity plateaus. This indicates that predominately all vacancies were annihilated in the first 12 hours. The lack of vacancies caused the diffusion rate of the solute to decrease after 12 hours.

The effect of natural aging time on 7075 and 7050 was also examined using DSC. The results are shown in Figure 3. As before, there were generally four distinct regions. The first region was associated with GP Zone formation. The second region was indicative of η' and η formation. The third region was η dissolution, with the fourth region was the peak associated with S phase (Al_2CuMg) dissolution.

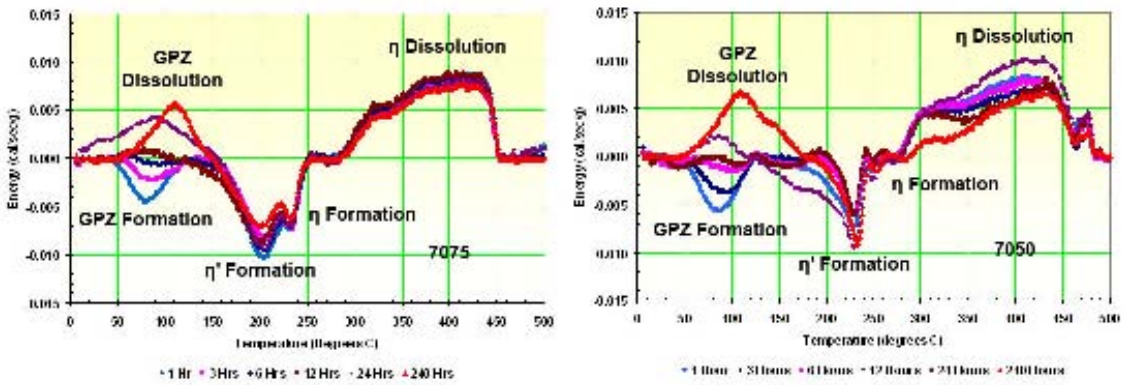

Figure 3. Effect of natural aging on the DSC Thermograms of 7075 and 7050.

For 7075, in the first region, attributed to GP Zone formation or dissolution, at times less than 12 hours, as the natural aging time increased, the peak temperature of GP Zone formation increased, indicating that the number of vacancies was being depleted, and the reaction required increased thermal activation. The range decreased as the natural aging time increased. As the natural aging time was increased, the amount of GP Zones formed during the DSC scan decreased. This indicates that the transformed fraction of GP Zones present was increasing with natural aging. There was little effect of natural aging time on the peak temperatures of Regions II and III, at times less then 12 hours.

This implies that at times less than twelve hours, nucleation and growth of GP Zones occur. At approximately 12 hours, all the vacancies have been consumed. After twelve hours, existing GP Zones grow at the expense of smaller or less stable GP Zones. Initially there is a large size distribution. As the small GP Zones revert or are absorbed, the size distribution decreases with increasing time and the size of the GP Zones grow with increasing time.

At t ≈ 12 hours, the volume fraction of GP Zones forming is approximately equal to the amount of GP Zones dissolving. At times greater than or equal to 12 hours, the peaks became endothermic, showing greater dissolution with increasing time, with a wide temperature range that decreases with natural aging time. This suggests that no new GP Zones are formed during the DSC scan, and that the number of GP Zones is decreasing with natural aging time. However, the GP Zones that remain are larger and more stable.

The increased area under the endothermic peaks suggests that a greater fraction of GP Zones were present as the natural aging time was increased during the DSC scan. It was likely that some GP Zones were growing at the expense of others because of the large size differences, indicated by the large temperature ranges. In Region II, the amount of η' and η present were generally constant as a function of increasing natural aging times. This indicates that there was increased amounts of η' precipitation occurring during natural aging. There was some possible transformation of GP Zones to η' as the natural aging time is increased past

12 hours. An incubation time was apparent before the GP Zones grow to an adequate size to precipitate η'.

Aluminum alloy 7050 exhibited a similar behavior to 7075. Region I was exothermic, and showed an increasing amount of GP Zones formed as a function of time. At a time slightly greater than 12 hours, the amount of GP Zones formed during the DSC scan was equal to the amount of GP Zones dissolved as the temperature was increased. As the aging time was increased, the peaks in Region I become endothermic and showed increased GP Zone dissolution. This indicates that more GP Zones were present. No natural aging effects were observed in Regions II and III.

From,[54] the area under the curve of either an endothermic or exothermic peak in a DSC scan is proportional to the volume fraction participating in formation or dissolution. Therefore it would be expected that the Region I area would show a progressive increase in the area associated with GP Zone formation or dissolution. An increase in the area under the curve was observed for the endothermic region. A gradual increase in the area under the formation peaks was observed. The shapes of the curves in Figure 4 for both 7075 and 7050 were similar, and show a sigmoidal increase, and indicate that a similar mechanism related to the growth and formation of GP Zones were occurring in each alloy. Increases in the delay before aging time and decreases in the first stage heating rate have been shown[55] to improve the properties at slow quench rates.

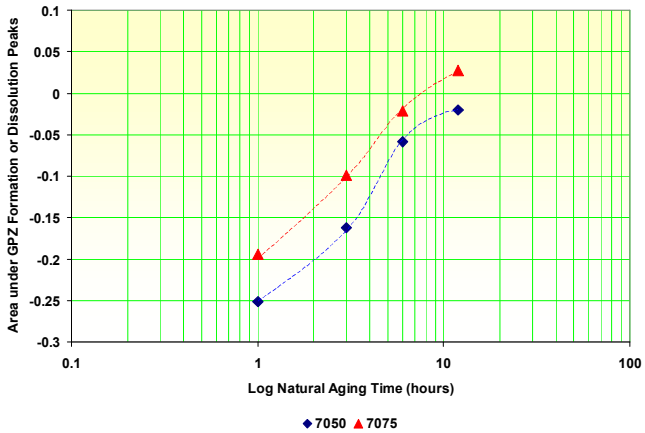

Figure 4. Volume fraction of GPZ from the area under the DSC formation and dissolution peaks.

DISCUSSION

Examination of the kinetics of GP zone formation during natural aging was accomplished using the Avrami equation:[51-52]

$$V_f = 1 - \exp\left[-(kt)^n\right]$$

where V_f is the fraction transformed, k is the rate constant (sec-1) and n is the Avrami time exponent.

Using the as-quenched hardness of 7075 and 7050 from Figure 1 and Figure 2 for ρ_i, and the peak-aged hardness of 205HV for ρ_0, the fraction transformed during natural aging was calculated.

Interestingly, the plateaus indicated in the hardness plots are shown more dramatically in the Avrami Plots (Figure 5). These plots show that the volume fraction increases steadily for approximately 12 hours after quenching, then plateaus

for approximately 18 hours, then increases steadily again at the same rate as before. This suggests that either a different precipitate has formed, and is growing at the same rate as the GP Zones.

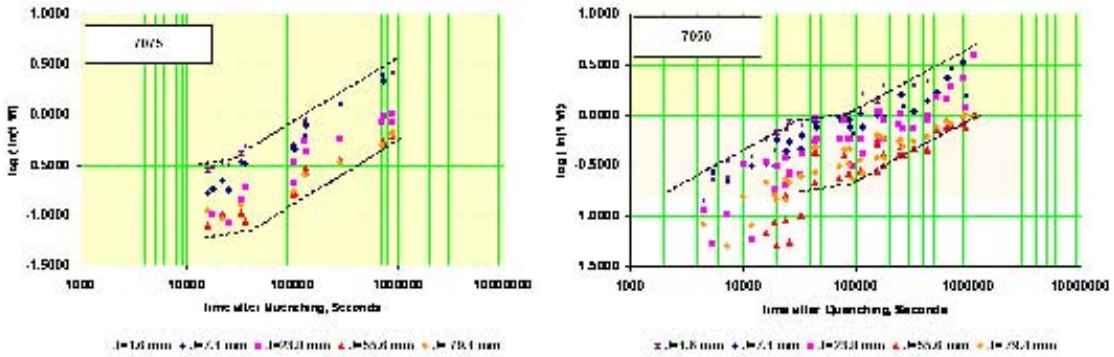

Figure 5. Avrami plot of the changes in fraction transformed, calculated from hardness, during natural aging of 7075 and 7050.

As can be seen from the plotted values of V_f versus time for 7075 and 7050 (Figure 5), the Avrami exponent, n, is the same for either alloy at the later regions of hardening, with n ≈ 0.5. This value of the Avrami exponent corresponds to spherical growth in the absence of impingement, when all nucleation sites are present at t = 0.[56] This exponent is also characteristic of parabolic growth. This value makes sense in view of the accepted understanding of GP zones in Al-Zn-Mg-Cu alloys.[57]

It was also observed that the Avrami exponent for hardening was the same regardless of the quench rate. This indicates that GP zones are present after all quench rates, and grow at the same rate. However, the quantity of GP zones decreases with decreasing quench rate. This decrease is due to the limited number of vacancies and vacancy-rich-clusters (VRC) present at low quench rates, and the low supersaturation of solute that occurs at slow quench rates. The mechanism for hardening during natural aging is the same for all quench rates, because of the Avrami exponent for hardening was the same for all quench rates. This is true for even the quench sensitive 7075 alloy.

The similarity of the slopes between the fast and slow quenched end of the Jominy End Quench specimen suggests that the mechanism of hardening is similar. However, the available quantity of hardening agents is different. At the fast-quenched end, there is a maximum supersaturation of solute. The driving force for the creation of GP zones is great. In addition, the amount of vacancies available for diffusion is also the greatest.

At the slow quenched end, there is a reduced amount of solute available for precipitation, and a reduced amount of vacancies. This reduction of solute and vacancies reduces the amount of hardening that occurs. However, the hardening Avrami exponent is similar in either the fast or slow cooled ends of the Jominy End Quench.

However, the change in hardness between the fast-quenched end and the slow quenched end is much smaller in 7050 than 7075 under identical conditions. This would indicate that either more solute is retained into solid solution over a broad range of quench rates, or that more vacancies are retained over a broad range of quench rates.

The natural aging response of 7050 exhibited a gradual increase in the hardness, followed by a plateau, then a gradual increase in the hardness. The Avrami exponents for the increases in hardness on either side of the plateau were

equivalent suggesting that the same mechanism was responsible for the increase in hardness. The shape of the curves can be explained by a gradual incubation time for vacancy rich clusters to form, with the formation of GP Zones occurring simultaneously. As more GP Zones are formed, the smaller zones revert, or are absorbed by larger GP Zones. This produces a net effect of a plateau in the hardness. The second increase in the hardness is from the growth of η'.

The 7075 natural aging response exhibited a gradual increase in hardness, followed by an increased rate of hardening. In this alloy, the shape of the curve suggests that there is a gradual increase in hardness due to clustering of vacancies, followed by the increase in hardness due to the formation of GP Zones.

This is evidenced by the changes in conductivity during natural aging. As the 7050 specimens naturally aged, the conductivity showed an initial plateau, followed by a decrease in conductivity. This decrease in conductivity was followed by another plateau in conductivity. In naturally aged 7075, there was an initial decrease in conductivity, followed by a conductivity plateau.

This data, along with the DSC data, suggests that all the vacancies have been consumed during growth to the first plateau. The data also suggests that in 7050, extended natural aging times causes the precipitation of η', while in 7075, only GPZ are formed.

CONCLUSIONS

Examination of the interaction of natural aging and quench rate showed that the natural aging time prior to artificial aging was critical for obtaining properties. An examination of the kinetics suggested that the kinetics correspond to spherical growth in the absence of impingement, when all nucleation sites are present at the beginning of transformation. Decreases in the Avrami-Mehl index as a function of quench rate was explained as being related to the amount of vacancies trapped during quenching. As the quench rate is decreased, the amount of vacancies also decreases. DSC and conductivity results indicate that the vacancies are consumed within the first 12 hours of natural aging. This effects the diffusion rate, and hence the formation of GP Zones.

The natural aging response of 7075 and 7050 differed. In 7075, it was found that initial clustering was followed by the formation and growth of GP zones. No evidence for the formation of η' was observed. In 7050, the sequence of clustering followed by GP Zone formation was also observed. However, it was also observed that at long natural aging times, the precipitation of η' occurred. These observations conflict with those of Staley[58] who indicated that only the formation of GP Zones occurs during natural aging of 7050.

REFERENCES

1 Hatch,J.E., *Aluminum: Properties and Physical Metallurgy*, ASM (Metals Park:1984) 154.
2 Grossman, M.A., *Metal Progress*, **4** (1938) 373.
3 Scott, H., *"Quenching Mediums," Metals Handbook*, ASM (1948) 615.
4 Wever, F., Archiv fűr das Eisenhűttenwesen, **5** (1936) 367.
5 Dakins, M., Central Scientific Laboratory, Union Carbide, Report CSL-226A.
6 Fink, W. L., Wiley, L. A., *Trans. AIME* **175** (1948) 414.
7 Suzuki, H., Kanno, M., Saitoh, H., *Keikinzoku* **33** 1 (1983) 29.
8 Piercy, G.R., Whitton, J.L., *J. Inst. Met.* **90** (1961) 386.

9 Watanabe, K., Yoshida, S, *Jap. J. Applied Physics* **19** 2 (1980) 219.
10 Kamigaki, N. Hashimoto, E., Deguchi, Y., *et al*, *Point Defects and Defect Interactions in Metals* (1982) 730.
11 Panseri, C., Federighi, T., *Acta Met.* **11** (1963) 575.
12 Watanabe, K., Yoshida, S, *Jap. J. Applied Physics* **19** 2 (1980) 219.
13 Panseri, C., Federighi, T., *Acta Met.* **11** (1963) 575.
14 Schmalzreid, H., Gerold, V., *Z. Metallkd*. **49** (1958) 291.
15 Gerold, V., Haberkorn, H., *Z. Metalk.*, **5**0 (1959) 568.
16 Polmear, I.J., *J. Inst. Met.* **87** (1958) 24.
17 Polmear, I. J., *J. Inst. Metals*, **86** (1957) 113.
18 Ryum, N., *Z. Metallkd*., **65** (1975) 338.
19 J.D. Embury, R.B. Nicholson, *Acta Met*. **13** (1965) 403.
20 H.A. Holl, *J. Met. Sci*. **1** (1967) 111.
21 Prabhu, N., Howe, J.M., *Met. Trans. A* **23A** 1 (1992) 135.
22 Bouquet, R., Auger, P., Bernole, M., Graf, R., *Memoires et Etudes Scientifiques Revue de Metallurgie*, **10** (1981) 539.
23 Gerold, V., Haberkorn, H., *Z. Metalk.*, **5**0 (1959) 568.
24 Guinier, A., *Compt. Rend*., **204** (1937) 1115.
25 Guinier, A., *Nature*, **142** (1938) 669.
26 Preston, G.D., *Proc. Royal Soc. A*, **166** (1934) 572.
27 Preston, G.D., *Nature* **142** (1938) 570.
28 Zhaoqi, L., Chungming, L., Gang, Z., Huongqiang, R., *Aluminum* (1986) 446 .
29 Zahra, A., Zahra, C. Y., Laffitte, M., *et al., Z. Metall.* **70** (1979) 172.
30 Zahra, A., Zahra, C. Y., Laffitte, M., *et al., Z. Metall.* **70** (1979) 172.
31 Asano, K., Abe, M., Fujiwara, A., *Mat. Sci. Eng.* **22** (1976) 61.
32 Staley, J.T., *Met. Trans.*, **5** (1974) 929.
33 Kovacs-Csetenyi,, E.Groma, G., Lendvai, J., *et al. Aluminum* **57** (1981) 472.
34 Cottrell, A., Bilby, B., *Proc. Phys. Soc. London, Sect A*, **268** (1962) 198.
35 Mukhopadhyay, A., *Phil. Mag*., **70** (1994) 135.
36 Bardhan, P., Starke, E., *J. Mat. Sci.*, **3** (1968) 577.
37 Holl, H.A., *J. Inst. Metals.* **93** (1964) 364.
38 Lorimer, G.W., Nicholson, G.B., *Acta Met.***14 (**1966) 1010.
39 Archambault, P., Moreaux, F., Beck, G., *ICSMA, 7e*, 12-16 August (1985) 589.
40 Bernole, M., Graf, R., *Mem. Sci. Rev. Met*., **69** (1972) 123.
41 Hyatt, M.V. , *Proc. Int. Conf. Aluminum Alloys*, Torino, Italy, October 1976.
42 Ryum, N., *Z. Metallkd*., **65** (1975) 338.
43 Bergman, G., Waugh, L., L. Pauling, *Nature* **169** (1952) 1057.
44 Suzuki, H., Kanno, M., Saitoh, H., *Keikinzoku*. **33** 7 (1983) 399.
45 Pashley, D.W., Jacobs, M.H., Vietz, J.T., *Phil. Mag*. **16** (1967) 51.
46 Mondolfo, L.F., Gjostein, N.A., Lewisson, *TAIMME* **206** (1956) 1378.
47 Thomas, G. Nutting, J. *J. Inst. Met.* **88** (1959) 81.
48 Loffler, H., Kovacs, I., Lendvai, J., *J. Mat. Sci.* **18** (1983) 2215.
49 Graf, R. *Compt. Rend*. **242** (1956) 1311.
50 Wilson, R.N., Moore, D.M., Forsyth, P.J.E., *J. Inst. Met.* **95** (1967) 177.
51 Johnson, W.A., Mehl,R.F., *Trans. AIME* **135** (1939) 416.
52 Avrami, M., *J. Chem. Phys.*, **7** (1940) 1103.
53 Mittemeijer, E.J., *J. Mat. Sci*., **27** (1992) 3977.
54 Deiasi, R., Adler, P., *Met. Trans.*, **8A** (1977) 1177.
55 Newkirk, J., MacKenzie, D.S., *J. Material Performance and Evaluation*, ASM, **9** 4 (2000) 408.
56 Christian, J.W., *Transformation in Metals and Alloys*, (Pergamon: Oxford), 1975, 536.
57 Lyman, C.E. and Vander Sande, J.B., *Met. Trans A*, **7A** (1976) 1211.
58 Staley. J.T., *Mat. Sci. Tech.* 3 11 (1987) 923.